

# Structural Characterizations of Two Synthetic Ni-Ludwigites, and Some Semiempirical EHTB Calculations on the Ludwigite Structure Type

R. Norrestam,<sup>\*1</sup> M. Kritikos,<sup>\*</sup> K. Nielsen,<sup>†</sup> I. Sjøtofte,<sup>†</sup> and N. Thorup<sup>†</sup>

<sup>\*</sup>Department of Structural Chemistry, Arrhenius Laboratory, Stockholm University, S-10691 Stockholm, Sweden; and  
<sup>†</sup>Structural Chemistry Group, Chemistry Department B, DTH 301, The Technical University of Denmark, DK-2800 Lyngby, Denmark

Received October 14, 1992; in revised form September 17, 1993; accepted September 21, 1993

The structures of two novel synthetic nickel-containing borates, Ni<sub>2</sub>CrO<sub>2</sub>BO<sub>3</sub> and Ni<sub>2</sub>VO<sub>2</sub>BO<sub>3</sub>, have been investigated by single crystal X-ray diffraction techniques and shown to have the ludwigite structure. The space group symmetry of both borates is *Pbam* with *Z* = 4. The unit cell dimensions are *a* = 9.209(1), *b* = 12.121(1), and *c* = 2.9877(3) Å for the Ni,Cr-borate, and *a* = 9.199(2), *b* = 12.211(2), and *c* = 2.988(1) Å for the Ni,V-borate. The structural model of the Ni,Cr-ludwigite has been refined on the basis of the 575 most significant (*I* > 3σ(*I*)) reflections with sin(θ)/λ ≤ 0.9 Å<sup>-1</sup> to an *R*-value of 0.029. For the Ni,V-ludwigite refinement, the 617 most significant (*I* > 3σ(*I*)) reflections with sin(θ)/λ ≤ 0.8 Å<sup>-1</sup> yielded an *R*-value of 0.023. Although the scattering powers of the cation pairs Ni/Cr and Ni/V are very similar, the refined cation distributions at the mixed metal sites yield approximately electroneutral compounds. The observed structural arrangement with the higher charged cations coplanar to the borate anion planes in the crystal structure is apparently a salient feature for all members of the pinakiolite structure family. A general model for the ludwigite structure, with alternating metal charges along the walls of octahedra, is supported by some semiempirical extended Hückel electronic band calculations performed on the homometallic Fe- and Co-ludwigites. © 1994 Academic Press, Inc.

## INTRODUCTION

Many metal borates with the general formula (*M'*, *M''* . . .)<sub>3</sub>O<sub>2</sub>BO<sub>3</sub>, where the metal ions (*M'*, *M''* . . .) can be di- to pentavalent, crystallize with the ludwigite structure. This structure type belongs to the pinakiolite family, in which all members have the same composition, (*M'*, *M''* . . .)<sub>3</sub>O<sub>2</sub>BO<sub>3</sub>. The members of this family may in general be considered to be different chemical twins of the parent structure of pinakiolite (1, 2, 3), with ludwigite as the simplest twin member of the family. With increasing structural complexity but maintaining the same general composition, the known pinakiolite members are pinakiolite, ludwigite, orthopinakiolite, takéuchiite, and blatterite.

<sup>1</sup> To whom correspondence should be addressed.

The present paper describes the syntheses and the structural details of two nickel ludwigites, Ni<sub>2</sub><sup>2+</sup>*M*<sup>3+</sup>O<sub>2</sub>BO<sub>3</sub> with *M*<sup>3+</sup> = Cr<sup>3+</sup> and V<sup>3+</sup>.

## EXPERIMENTAL

### Syntheses

The title compounds were synthesized by heating stoichiometric mixtures of metal oxides (NiO, Cr<sub>2</sub>O<sub>3</sub>, and V<sub>2</sub>O<sub>5</sub> used as oxide sources) with a slight excess (≈5%) of B<sub>2</sub>O<sub>3</sub> in air at 1000°C in open Pt tubes. After the initial heat treatment, another 10% B<sub>2</sub>O<sub>3</sub> was added to the mixtures. The mixtures were heated to 1200°C and slowly cooled (17°/hr) to 600° before the furnaces were turned off. X-ray powder photographs indicated that the obtained product of the Ni,Cr-ludwigite synthesis, apart from ludwigite as a major phase, also contained small amounts of NiO. For the Ni,V-ludwigite synthesis, the minor phase was Ni<sub>3</sub>(VO<sub>4</sub>)<sub>2</sub>. The obtained Ni,V-ludwigite sample contained single crystals of a size suitable for X-ray studies. The Ni,Cr-ludwigite sample had to be recrystallized by heating it to 1200°C with a large excess of borax as a flux medium, followed by a cooling treatment as described above. Alternatively, these two ludwigites can also be prepared by using Ni powder instead of NiO in the initial synthesis stage.

### X-Ray Diffraction Studies

The possible space group symmetry *Pbam* (or *Pba2*), in agreement with that found for other ludwigites (see, e.g., (4)), was deduced from the observed systematic absences and the symmetry of the X-ray intensity data. The choice of the centrosymmetric space group *Pbam* was supported by the result of the structural refinements. The X-ray diffraction data collected with a single crystal diffractometer were corrected for background, Lorentz, polarization, and absorption effects. To check the validity of the numerically estimated transmission factors, the de-

viations of the intensities collected at a range of different  $\psi$  values for about 10 different reflections were statistically analyzed. With the use of a computer program, CADPSI, written by one of the authors (R.N.), the intensity variations, as represented by the  $\chi^2$  values for each reflection, were shown to become insignificant (95% confidence level) after the absorption corrections. Further numerical details of the experimental conditions and the structural refinements are given in Table 1. Recently, Bluhm and Müller-Buschbaum published (5) unit cell dimensions of a powder specimen of  $\text{Ni}_2\text{CrO}_2\text{BO}_3$ , which agree within  $5 \cdot \sigma$  with those obtained in the present study.

During the refinements of the structural parameters, the total metal occupancies at each metal position were assumed to be 100%. In the initial stages, the ratios Ni:Cr and Ni:V were allowed to vary without any constraints applied. However, as a Ni occupancy of 100% was obtained for the  $M(1)$  position of the Ni,Cr-ludwigite structure, this position was treated as a pure Ni position in the subsequent refinements. The metal compositions obtained for the two ludwigites are  $\text{Ni}_{1.94(4)}\text{Cr}_{1.06(4)}\text{O}_2\text{BO}_3$  and  $\text{Ni}_{1.82(4)}\text{V}_{1.18(4)}\text{O}_2\text{BO}_3$ , reasonably close to the composition  $M'_{2.00}M''_{1.00}\text{O}_2\text{BO}_3$  expected for divalent  $M' = \text{Ni}$  and trivalent  $M''$  metal ions. The deviations from the ideal composition are so small ( $<5 \cdot \sigma$ ) that they are probably insignifi-

TABLE 1  
Experimental Conditions for the Crystal Structure Determinations of  $\text{Ni}_2\text{CrO}_2\text{BO}_3$  and  $\text{Ni}_2\text{VO}_2\text{BO}_3$

Name	Ni,Cr-ludwigite	Ni,V-ludwigite
Formula	$\text{Ni}_2\text{CrO}_2\text{BO}_3$	$\text{Ni}_2\text{VO}_2\text{BO}_3$
Formula weight	260.2	259.2
Space group	<i>Pbam</i>	<i>Pbam</i>
Unit cell dimensions	$a = 9.209(1), b = 12.121(1), c = 2.9877(3) \text{ \AA}$	$a = 9.199(2), b = 12.211(2), c = 2.988(1) \text{ \AA}$
Unit cell volume ( <i>V</i> )	$333.49(6) \text{ \AA}^3$	$335.6(1) \text{ \AA}^3$
Formula units per cell ( <i>Z</i> )	4	4
Calculated density ( <i>D<sub>c</sub></i> )	$5.182 \text{ g} \cdot \text{cm}^{-3}$	$5.130 \text{ g} \cdot \text{cm}^{-3}$
Radiation	MoK $\alpha$	MoK $\alpha$
Wavelength ( $\lambda$ )	$0.71073 \text{ \AA}$	$0.71073 \text{ \AA}$
Temperature ( <i>T</i> )	293(1) K	293(1) K
Crystal shape	Needle	Needle
Crystal size	$0.02 \times 0.02 \times 0.06 \text{ mm}$	$0.03 \times 0.03 \times 0.07 \text{ mm}$
Diffractionmeter	Enraf-Nonius CAD4	Enraf-Nonius CAD4
Determination of unit cell		
Number of reffs. used	24	20
$\theta$ -range	13.0 to 16.4°	8.0 to 13.5°
Intensity data collection		
Maximum $\sin(\theta)/\lambda$	$0.904 \text{ \AA}^{-1}$	$0.807 \text{ \AA}^{-1}$
Range of <i>h, k, and l</i>	0 to 16, -21 to 21, and 0 to 5	0 to 14, 0 to 19, and 0 to 4
Standard reflections	2	2
Intensity instability	<2%	<2%
Total number of reffs.	2306	851
Internal $R_{\text{int}}$ value	0.044	—
Number of unique reffs.	1181	851
Number of observed reffs.	575	617
Significance criterion	$I > 3 \cdot \sigma(I)$	$I > 3 \cdot \sigma(I)$
Absorption correction		
Linear absorption coeff.	$142.6 \text{ cm}^{-1}$	$137.1 \text{ cm}^{-1}$
Transmission factor range	0.70 to 0.77	0.68 to 0.73
Structure refinement		
Minimization of	$\Sigma w \cdot \Delta F^2$	$\Sigma w \cdot \Delta F^2$
Anisotropic model	Metal atoms	Metal atoms
Isotropic model	B and O atoms	B and O atoms
Refined parameters	43	43
Weighting scheme	$(\sigma^2(F) + 0.0003 F ^2)^{-1}$	$(\sigma^2(F) + 0.0003 F ^2)^{-1}$
Final <i>R</i>	0.029	0.023
Final $wR$	0.030	0.028
Final $wR$ for all reffs.	0.059	0.053
Final $(\Delta/\sigma)_{\text{max}}$	0.001	0.001
Final $\Delta\rho_{\text{min}}$ and $\Delta\rho_{\text{max}}$	-1.5 and $1.4 \text{ e}^{-}/\text{\AA}^3$	-1.1 and $1.0 \text{ e}^{-}/\text{\AA}^3$

TABLE 2  
Fractional Atomic Coordinates ( $\times 10^4$ ) and Thermal Parameters ( $\times 10^4 \text{ \AA}^2$ ) for the Nickel–Chromium Ludwigite and the Nickel–Vanadium Ludwigite Structures

Cr occupancy	Atom	<i>x</i>	<i>y</i>	<i>z</i>	$U_{11}$	$U_{22}$	$U_{33}$	$U_{12}$
0 %	<i>M</i> (1)	0	0	1/2	39(3)	42(3)	55(4)	−3(4)
11(2)	<i>M</i> (2)	0	1/2	0	48(3)	42(4)	48(4)	−(4)
88(2)	<i>M</i> (3)	2398(1)	1136(1)	0	30(3)	32(2)	31(3)	−1(3)
6(2)	<i>M</i> (4)	4991(1)	2191(1)	1/2	38(2)	41(2)	44(3)	−6(3)
	O(1)	6220(4)	1397(4)	0	45(6)			
	O(2)	−1517(4)	411(3)	0	48(6)			
	O(3)	1084(4)	1424(4)	1/2	64(6)			
	O(4)	3452(5)	2615(3)	0	58(7)			
	O(5)	3828(4)	765(3)	1/2	51(7)			
	B	7719(6)	1400(5)	0	38(9)			
V occupancy	Atom	<i>x</i>	<i>y</i>	<i>z</i>	$U_{11}$	$U_{22}$	$U_{33}$	$U_{12}$
28(2)%	<i>M</i> (1)	0	0	1/2	43(3)	57(3)	65(3)	−6(2)
10(2)	<i>M</i> (2)	0	1/2	0	54(3)	46(3)	59(3)	−1(2)
75(2)	<i>M</i> (3)	2395(1)	1136(1)	0	39(2)	46(2)	54(2)	−2(2)
6(2)	<i>M</i> (4)	5001(1)	2180(1)	1/2	42(2)	45(2)	63(2)	−4(1)
	O(1)	6238(3)	1406(2)	0	63(4)			
	O(2)	−1505(3)	419(2)	0	74(5)			
	O(3)	1099(3)	1438(2)	1/2	90(5)			
	O(4)	3483(3)	2623(2)	0	67(5)			
	O(5)	3833(3)	769(2)	1/2	74(5)			
	B	7737(4)	1399(3)	0	55(6)			

Note. The scattering factors used for refining the structures were linear combinations of neutral atoms for each metal position (cf. Table 3), constrained to give occupancies that add up to 100% at each position. The anisotropic temperature factor expression (space group *Pbam*) used is  $\exp[-2\pi^2((ha^*)^2U_{11} + \dots + 2hka^*b^*U_{12})]$ .

cant. Accordingly, the vanadium content in the Ni,V-ludwigite was assumed to be pure trivalent and the compositions of both ludwigites were constrained in the final refinements to become ideal  $(\text{Ni}_2\text{MO}_2\text{BO}_3, M = \text{Cr or V})$ . The final atomic coordinates and thermal parameters obtained are listed in Table 2 and the relevant metal–oxygen bond distances in the coordination octahedra are given in Table 3.

The structural refinements were carried out by means of the SHELX-76 package (6) locally modified for an IBM PS/2-80 personal computer, using atomic scattering factors from the "International Tables for X-ray Crystallography" (7). The polyhedral packing diagrams were obtained with the program ATOMS (8).

#### Electronic Band Calculations

The band calculations were performed with the semi-empirical extended Hückel tight binding (EHTB) method (cf. (9)), using the program (QCPE No. 571) written by Whangbo *et al.* (10). The parameters used (Table 4) were those given in the compilation by Alvarez (11). The algorithm developed by Monkhorst and Pack (12) was applied to map the *k*-space. A set of 64 *k*-points in the irreducible

wedge of the primitive orthorhombic Brillouin zone was used in all calculations. No charge iterations on the  $H_{ii}$  values were performed.

#### DISCUSSION

In the ludwigite structure, the oxygen coordination octahedra around the metal ions (Fig. 1) are linked together in the crystal structure by edgesharing to form five-octahedra-wide flat walls (denoted F walls by Takéuchi (2)) and zigzag walls. The walls consist of columns of octahedra around the metal positions *M*(1), *M*(3), and *M*(4). Due to the inversion centers (cf. Fig. 1) at *M*(1), the F walls have the following sequence of metal positions: *M*(4)–*M*(3)–*M*(1)–*M*(3)–*M*(4). The columns formed by the central coordination octahedra of the zigzag walls, viz., those around the *M*(2) and *M*(3) metal positions (Fig. 1), form three-octahedra-wide walls (denoted C walls by Takéuchi (2)), as the *M*(2) positions are at inversion centers. The walls extend in the *c* direction and the triangular borate groups fill the voids between the walls and are linked to these by cornersharing. The other members of the pinakolite family have similar structural arrange-

TABLE 3  
Metal–Oxygen Bond Distances (with e.d.s.'s) and Multiplicities in the Coordination Octahedra of the Nickel–Chromium and of the Nickel–Vanadium Ludwigites

Distances				
Atoms	Mult.	Ni,Cr-ludwigite	Ni,V-ludwigite	Expected type
M1–O(2)	4	2.105(4)	2.101(3)	Long
–O(3)	2	1.995(4)	2.027(3)	Short
M2–O(1)	2	2.032(4)	2.060(3)	
–O(5)	4	2.064(4)	2.066(3)	
M3–O(2)	1	2.044(4)	2.069(3)	
–O(3)	2	1.954(4)	1.947(3)	Short
–O(4)	1	2.038(4)	2.074(3)	
–O(5)	2	2.042(4)	2.046(3)	
M4–O(1)	2	2.108(4)	2.102(3)	Long
–O(3)	1	1.958(4)	1.967(3)	Short
–O(4)	2	2.123(4)	2.116(3)	Long
–O(5)	1	2.034(4)	2.031(3)	
B–O(1)	1	1.381(6)	1.379(4)	
–O(2)	1	1.391(6)	1.385(4)	
–O(4)	1	1.371(6)	1.378(4)	

Note. The expected type of bond lengths is based on the common trends of ludwigite structures discussed in the present paper.

ments, but with different widths of the walls (see, e.g., (3, 13, 14)).

From Table 2, it is evident that the major  $M^{3+}$  content in both ludwigites is located in the  $M(3)$  position (common to the F and C walls), while the other metal positions all have major  $M^{2+}$  contents. As the metal sequences across the F and the C walls are  $M(4)$ – $M(3)$ – $M(1)$ – $M(3)$ – $M(4)$  and  $M(3)$ – $M(2)$ – $M(3)$ , respectively, both types of walls have alternating metal ion charge distributions. Such distributions are common not only for ludwigites but for the pinakiolite family of structures in general (3, 15, 16, 17). The metal–metal contacts between adjacent edge-sharing columns of octahedra are all  $\geq 3.0$  Å, except for the  $M(2) \cdots M(3)$  contacts, which are 2.79 Å (see discussion

below). Due to the short  $c$  axis of ludwigites, the metal–metal contacts along each column are 2.99 Å.

The  $M^{3+}$  content at the  $M(4)$  position is particularly low in both ludwigites, giving formal metal ion charges close to +2.0. Besides belonging to the F wall, the columns of octahedra around the  $M(4)$  position can be considered to be corner columns, frequently denoted S columns (2), in the zigzag walls. Metal ions in the S columns of pinakiolites have generally been observed to have low formal charges.

The average metal–oxygen bond lengths (Table 3) in the coordination octahedra are very similar for the Ni,Cr- and Ni,V-ludwigites. For the  $M(1)$ ,  $M(2)$ , and  $M(4)$  positions, the range of the averages is 2.05 to 2.08 Å. The

TABLE 4  
Extended Hückel Parameters

Atom	Orbital	$H_{ii}$ (eV)	$\zeta_1$	$c_1$	$\zeta_2$	$c_2$
B	2s	–15.2	1.3			
	2p	–8.5	1.3			
O	2s	–32.3	2.275			
	2p	–14.8	2.275			
Co	4s	–9.21	2.0			
	4p	–5.29	2.0			
	3d	–13.18	5.55	(0.5680)	2.10	(0.6060)
Fe	4s	–9.10	1.9			
	4p	–5.32	1.9			
	3d	–12.6	5.35	(0.5505)	2.00	(0.6260)

Note.  $H_{ii}$  is the effective potential,  $\zeta$  the Slater type orbital exponents, and  $c$  the coefficients used in double  $\zeta$ -expansion.

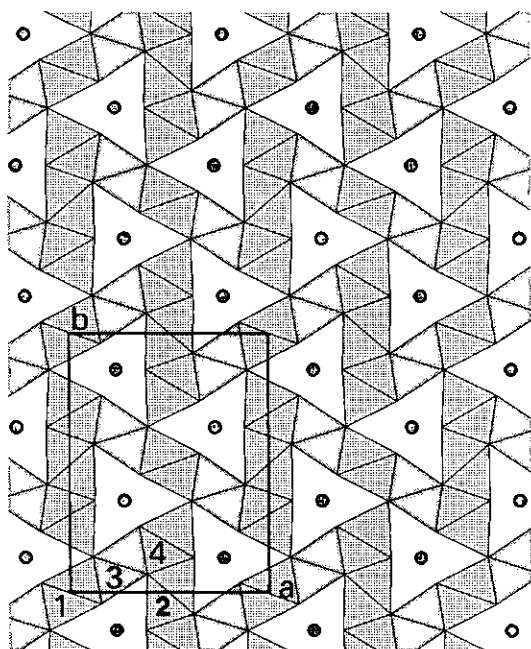


FIG. 1. Polyhedral drawing of the ludwigite structure viewed along the  $c$  axis; the  $a$  axis is horizontal,  $b$  is vertical, and the origin is at the lower left corner. The unit cell and the atom numbering used for the metal positions are indicated. Metal atoms numbers 1 and 2 are at inversion centers. The octahedra around metal positions number 3, where the major  $M^{3+}$  content is located, are indicated as dark gray. The boron atoms of the trigonal borate groups in the voids between the walls are drawn as filled circles.

shorter averages of the  $M(3)$ –O bonds (2.012 and 2.022 Å) are obviously due to the higher  $M^{3+}$  content. The ionic radii of  $Cr^{3+}$  and  $V^{3+}$  are both smaller than that of  $Ni^{2+}$  (cf. (18)). Empirical bond valences at the metal ion positions, estimated with the parameters and the bond valence–bond distance correlation functions given by Brown and Altermatt (19), become 1.9 to 2.0 valence units (v.u.) for the  $M(1)$ ,  $M(2)$ , and  $M(4)$  positions and 2.8 v.u. for the  $M(3)$  position.

The observed metal–oxygen bonds (Table 3) give estimated empirical bond valences (1.9 to 2.0 v.u.) for the oxygen atoms close to 2.00 v.u. The borate oxygen atoms (O(1), O(2), and O(4)) are all four-coordinated. Apart from the short covalent bonds (1.378 to 1.391 Å) to the boron atoms, the borate oxygen atoms are coordinated by two metal ions at longer distances of about 2.11 Å and by one metal ion at an intermediate distance of about 2.05 Å. The short bonds are formed to the higher charged  $M(3)$  metal atoms, which are within the planes of the borate ions. The longer bonds are formed out of these planes to the lower charged  $M(1)$  and  $M(4)$  metal atoms. The arrangement with the higher charged cations coplanar to the borate anion planes in the crystal structure is apparently a salient feature for all members of the pinakiolite structure family. In the absence of ions like  $Mn^{3+}$ , which

introduce pronounced structural perturbations due to Jahn–Teller effects, all members (15, 16, 20, 21) for which the radii of the higher charged ions are less than those of the lower charged ones will have a similar pattern (cf. above) of coordination distances around their borate oxygens. The two remaining oxygen atoms (O(3) and O(5)), not belonging to any borate group, are both located in the S columns of the zigzag chains, with O(3) forming the outer and O(5) the inner corners. The O(3) atoms, which link two zigzag chains together, are coordinated by four metal ions, while the O(5) atom is five-coordinated. The different coordinations around these two oxygen atoms are reflected by the shorter metal–O(3) distances.

Several transition metal oxide systems have been studied quite successfully (22) on the basis of the extended Hückel tight binding (EHTB) method for electronic band calculations. Although the method is very approximate, reasonable qualitative conclusions can in general be drawn from EHTB calculations. As the substitutional disorder in the present heterometallic ludwigites ( $Ni_2CrO_2BO_3$  and  $Ni_2VO_2BO_3$ ) is difficult to treat adequately, the calculations were performed on homometallic mixed-valence species. Preferably, the calculations ought to be carried out for idealized models of the structure. However, the structural features of the ludwigites impose steric constraints that preclude the derivation of a model with ideally octahedral metal coordination (same metal–oxygen distances) sharing oxygen atoms with trigonal borate ions. Thus, the experimental structural data for  $Fe_3O_2BO_3$  (20) and  $Co_3O_2BO_3$  (16) were chosen for the EHTB calculations.

The general features of the charge distributions at the metal sites from the EHTB calculations on the Fe- and Co-ludwigites agree well with the experimental results for the Ni,Cr- and Ni,V-ludwigites. Thus, alternating metal charge distributions are obtained along the C and F walls and a low charge is obtained at the S column metal site  $M(4)$ . The shortest metal–metal distances in all ludwigites are found between the  $M(2)$  and  $M(3)$  positions. These positions are located in two adjacent octahedra columns which have an edge (formed by two O(5) atoms) in common. As discussed by, *inter alia*, Goodenough (23) and Hay *et al.* (24), one condition for direct metal–metal interaction in such cases is that the metal–ligand–metal angle should be less than  $90^\circ$ . This condition is fulfilled in both ludwigites as the  $M(2)$ –O(5)– $M(3)$  angles are  $83.2^\circ$  (Fe) and  $84.0^\circ$  (Co). The  $M(2) \cdots M(3)$  distances in the two ludwigites are also of similar magnitude (2.79 Å), but the  $M(2) \cdots M(3)$  interaction for the Fe-ludwigite as judged by the EHTB crystal orbital overlap population (25), COOP, is larger (Table 5). The COOPs are  $\leq 0.01$  for all other metal–metal contacts in the two structures. The different unit cell valence electron counts of the two ludwigites imply occupation of crystal orbitals with higher

TABLE 5  
Calculated Charges for  $M$  ( $M = \text{Fe}, \text{Co}$ ), O, and B and Overlap Populations, OP, for M-M and M-O Interactions

$\text{Co}_3\text{O}_2\text{BO}_3$			$\text{Fe}_3\text{O}_2\text{BO}_3$		
Atom	Charge		Atom	Charge	
Co(1)	0.65		Fe(1)	0.63	
Co(2)	0.89		Fe(2)	1.51	
Co(3)	1.17		Fe(3)	0.96	
Co(4)	-0.67		Fe(4)	0.66	
O(1)	-0.83		O(1)	-0.82	
O(2)	-0.85		O(2)	-0.84	
O(3)	-0.67		O(3)	-0.79	
O(4)	-0.84		O(4)	-0.83	
O(5)	-0.85		O(5)	-0.87	
B	1.46		B	1.46	

Co-Co	Distance (Å)	OP	Fe-Fe	Distance (Å)	OP
Co(1)-Co(1)	3.026	-0.01	Fe(1)-Fe(1)	3.073	0.01
Co(1)-Co(3)	3.023	-0.01	Fe(1)-Fe(3)	3.101	-0.01
Co(2)-Co(2)	3.026	-0.01	Fe(2)-Fe(2)	3.073	0.01
Co(2)-Co(3)	2.788	0.00	Fe(2)-Fe(3)	2.787	0.06
Co(2)-Co(4)	3.086	-0.01	Fe(2)-Fe(4)	3.176	-0.01
Co(3)-Co(3)	3.026	-0.02	Fe(3)-Fe(3)	3.073	-0.01
Co(3)-Co(4)	3.124	-0.01	Fe(3)-Fe(4)	3.192	-0.01
Co(4)-Co(4)	3.026	0.00	Fe(4)-Fe(4)	3.073	0.01
Co(1)-O(2)	2.137	0.14	Fe(1)-O(2)	2.200	0.16
Co(1)-O(3)	2.001	0.26	Fe(1)-O(3)	2.036	0.26
Co(2)-O(1)	2.014	0.24	Fe(2)-O(1)	2.060	0.24
Co(2)-O(5)	2.076	0.18	Fe(2)-O(5)	2.105	0.20
Co(3)-O(2)	2.043	0.22	Fe(3)-O(2)	2.074	0.22
Co(3)-O(3)	1.960	0.28	Fe(3)-O(3)	2.008	0.28
Co(3)-O(4)	2.047	0.22	Fe(3)-O(4)	2.071	0.24
Co(3)-O(5)	2.075	0.20	Fe(3)-O(5)	2.092	0.20
Co(4)-O(1)	2.146	0.14	Fe(4)-O(1)	2.205	0.16
Co(4)-O(3)	1.959	0.30	Fe(4)-O(3)	1.956	0.32
Co(4)-O(4)	2.147	0.14	Fe(4)-O(4)	2.208	0.16
Co(4)-O(5)	2.059	0.22	Fe(4)-O(5)	2.102	0.22

Note. The OPs were evaluated at the highest occupied crystal orbital and normalized to one bond.

energy for the Co-ludwigite. Thus, the COOP curves (Fig. 2) of the  $M(2) \cdots M(3)$  contacts show that metal-metal antibonding states (negative overlap) are occupied for  $\text{Co}_3\text{O}_2\text{BO}_3$ , but not for  $\text{Fe}_3\text{O}_2\text{BO}_3$ . A significant  $M(2) \cdots$

$M(3)$  interaction (with intermediate oxidation states of +2.5 at the  $M(2)$  and  $M(3)$  positions) has been suggested by Swinnea and Steinfink (20) as an explanation of the features of Mössbauer spectra collected for  $\text{Fe}_3\text{O}_2\text{BO}_3$ .

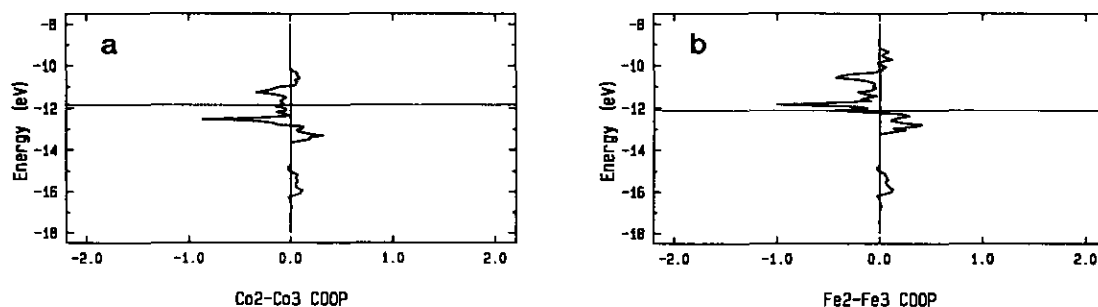


FIG. 2. Crystal orbital overlap population curves (COOP) in the Fe- and Co-ludwigites. The horizontal solid lines indicate the highest occupied crystal orbitals. (a) The Co(2)-Co(3) COOP in  $\text{Co}_3\text{O}_2\text{BO}_3$ ; (b) the Fe(2)-Fe(3) COOP in  $\text{Fe}_3\text{O}_2\text{BO}_3$ .

The COOPs show, as expected, that the  $3d$  orbitals on the transition metal ions combine with the oxygen  $2p$  orbitals to form metal–oxygen bands (from  $-17$  to  $-15$  eV). Small concentrations of metal–oxygen bands involving the oxygen  $2s$  orbitals and all metal valence orbitals occur at lower energies ( $-34$  to  $-32$  eV). The major metal–metal bonding states (Fig. 2) are located just below the highest occupied crystal orbitals ( $-12.06$  and  $-11.82$  eV).

#### ACKNOWLEDGMENTS

The present study was financially supported by the Swedish National Research Council. Some of the initial computations were performed on microVAX-II computer equipment financed by grants from the Danish Natural Science Research Council and from the Danish National Technical Research Council.

#### REFERENCES

1. S. Andersson and B. Hyde, *J. Solid State Chem.* **9**, 92 (1974).
2. Y. Takéuchi, *Recent Prog. Nat. Sci. Jpn.* **3**, 153 (1978).
3. R. Norrestam and J.-O. Bovin, *Z. Kristallogr.* **181**, 135 (1987).
4. Y. Takéuchi, T. Watanabé, and T. Ito, *Acta Crystallogr.* **3**, 98 (1950).
5. K. Bluhm and Hk. Müller-Buschbaum, *Z. Anorg. Allg. Chem.* **582**, 15 (1990).
6. G. M. Sheldrick, "SHELX-76, Program for Crystal Structure Determination." University of Göttingen, 1976.
7. "International Tables for X-Ray Crystallography," Vol. IV. Kynoch Press, Birmingham, 1974.
8. E. Dowty, "ATOMS, A Computer Program for Displaying Atomic Structures." Copyright 1989, Eric Dowty, 521 Hidden Valley Road, Kingsport, TN 37663.
9. M.-H. Whangbo and R. Hoffmann, *J. Am. Chem. Soc.* **100**, 6093 (1978).
10. M.-H. Whangbo, M. Evain, T. Hughbanks, M. Kertész, S. Wijeysekera, C. Wilker, C. Zheng and R. Hoffmann, "Quantum Chemistry Program Exchange," Program No. 571, 9 No. 2 (1989) 61. Indiana University, Bloomington, IN, 1989.
11. S. Alvarez, "Tables of Parameters for Extended Hückel Calculations." Universitat de Barcelona, unpublished, 1989.
12. H. J. Monkhorst and J. D. Pack, *Phys. Rev. B* **13**, 5188 (1976).
13. P. Moore and T. Araki, *Am. Mineral.* **59**, 985 (1974).
14. Y. Takéuchi, N. Haga, T. Kato, and Y. Miura, *Can. Mineral.* **16**, 475 (1978).
15. R. Norrestam, S. Dahl, and J.-O. Bovin, *Z. Kristallogr.* **187**, 201 (1988).
16. R. Norrestam, K. Nielsen, I. Sjøtofte, and N. Thorup, *Z. Kristallogr.* **189**, 33 (1989).
17. R. Norrestam and S. Hansen, *Z. Kristallogr.* **191**, 105 (1990).
18. R. D. Shannon, *Acta Crystallogr. Sect. A* **32**, 751 (1976).
19. I. D. Brown and D. Altermatt, *Acta Crystallogr. Sect. B* **41**, 244 (1985).
20. J. S. Swinnea and H. Steinfink, *Am. Mineral.* **68**, 827 (1983).
21. V. Alfredsson, J.-O. Bovin, R. Norrestam, and O. Terasaki, *Acta Chem. Scand.* **45**, 797 (1991).
22. E. Canadell and M.-H. Whangbo, *Chem. Rev.* **91**, 965 (1991).
23. J. Goodenough, "Magnetism and the Chemical Bond." Wiley, New York–London, 1963.
24. P. J. Hay, J. C. Thibeault, and R. Hoffmann, *J. Am. Chem. Soc.* **97**, 4884 (1975).
25. T. Hughbanks and R. Hoffmann, *J. Am. Chem. Soc.* **105**, 3528 (1983).